Spatial Signatures of Road Network Growth for Different Levels of Global Planning

Michelle T. Cirunay
Rene C. Batac
Physics Department, College of Science
De La Salle University
2401 Taft Avenue
Manila, Philippines

We compare the statistical distributions of the geometrical properties of road networks for two representative datasets under different levels of planning: the cities comprising Metropolitan Manila show the conditions under bottom-up self-organized growth, while Brasilia and the Australian Capital Territory centered at Canberra represent the case of strict top-down planning. The distribution of segmented areas of the cities shows a dual power-law behavior, with the larger areas following the ~1.9 scaling exponent observed in other cities, while the smaller areas show a lower exponent of ~0.5, believed to be due to practical considerations. While all cities are found to favor the formation of straight road segments, the planned city roads have a preponderance of sinuous roads, with sinuosities approaching π. A simple model based on a nearest-neighbor directed branching coupled with sectional grid formations is proposed to capture the nontrivial statistical features observed.

Keywords: cities; scaling phenomena; self-organization; computational techniques; rule-based models

1. Introduction

Cities are complex systems that are composed of a multitude of agents and their interactions [1, 2]. Among all the aspects of the urban fabric, the road networks, as almost-permanent spatial imprints of urban development [3], are very good examples of how seemingly uncorrelated mechanisms across various spatiotemporal scales result in the emergence of complex behavior [4]. At the planning level, the formation of individual roads is guided by various political, economic and social factors; on the ground, the local geography and other practical considerations shape the actual road structure. The interplay between central planning and local self-organization [5, 6] produces emergent properties of the resulting network, which can be quantified through the statistical analyses of the patterns they leave behind in space [7–9].

https://doi.org/10.25088/ComplexSystems.30.3.273

One of the most straightforward means of quantifying the spatial complexity is through fractal analysis [10–13], in view of the fact that roads are space-filling agents. These works are complemented by temporal analyses using long-period records of city road network evolution [14], showing that the pattern evolves from a multifractal to a monofractal state in time [15, 16]. Their network structure in space and their functions as transport architectures have also allowed for studies combining geometrical and topological characterizations using graph (network) theory [8, 17–20]. Such results have not only contributed to our understanding and modeling of road network evolution [21] but also provided practical applications, such as for planning transport and evacuation scenarios across the road network during disaster situations [22].

Studying the geometrical and topological properties of road network structures and comparing them with planar graph representations oftentimes reveal the combined effects of two independent forcing mechanisms that contribute toward the complexity of the resulting pattern. For example, Cardillo et al. [23] classified cities with various historical and socioeconomic backgrounds based on *efficiency* and *cost* as measured from two representative random planar networks, revealing some similarities and differences across the test subjects considered. Strano et al. [9] analyzed the roles of *densification* and *exploration* in the street network of Milan. The city road structure reveals a backdrop of older, more central roads flanked in time by less central roads, in a process that is believed to be at work in the historical development of most cities. Moreover, Barthelemy et al. [5] considered a period of *top-down planning* against the backdrop of *self-organization* in the historical development of Paris, revealing the roles of continuous growth and abrupt changes in the city growth.

The latter two factors are of particular interest to us, as the levels of planning and the conditions for self-organized growth may differ across cities, even for those under relatively similar conditions. We are in agreement with the observations of Strano et al. [9], who suggested that studies of this kind require further validation and comparison with different datasets from across varying geographical and economic constraints. In this work, therefore, our twofold goal is (*i*) to provide a comparison of the effects of strict planning and self-organization, and (*ii*) to do it for two datasets from very different backgrounds from those previously studied. On one hand, we present the data for the component cities of Metropolitan Manila, the capital region of the Philippines. The cities are geographically constrained, politically autonomous and economically disparate, which best illustrates self-organization at local scales even for a single contiguous area. On the other hand, we also collected data from two

conurbations that were drawn up from strict master plans: Brasilia, the capital region of Brazil, and Canberra, the capital region of Australia. Our quantitative analysis of the spatial features of these two classes of cities have revealed similarities and differences that are ultimately tied to the differences in the levels of their planning. A rule-based model that extends the previous work [24] based on the assumed physical rules on the ground is found to mimic the observed distribution of the self-organized Philippine cities.

2. Datasets and Methods

2.1 City Datasets

We investigate two general classes of cities and their conurbations, all of which are capital regions of their respective countries, based on the levels of planning and self-organization present during their development. For the predominantly self-organizing cities, we extract the road network structures of the 16 cities and one town in Metro Manila, the National Capital Region (NCR) of the Philippines, while for the cities that are drawn up from master plans, we considered the cases of the Australian Capital Territory (ACT), particularly near the highly planned city of Canberra and the Brasilia Federal District (BFD) in Brazil, centered around the city of Brasilia. Although we studied the general urban conurbation, for ease of naming convention, we refer to these regions based on the capital cities: Manila, Canberra and Brasilia, respectively.

The City of Manila has been the historical capital of the Philippines since the Spanish colonization in 1571. Attempts to move the capital were made in the late 1930s, with a new planned settlement that eventually became Quezon City [25]; the city, which is bigger in area and adjacent to Manila, became the capital from 1948 to 1976. In 1976, however, the designation of Manila as the capital was restored, and the Metropolitan Manila area, composed of the City of Manila, Quezon City and 15 other adjacent cities and towns, was created to be the NCR of the Philippines. Because of their independent histories, there is no centralized and coordinated plan for the conurbation during the growth and development of their road networks, making them good test subjects for illustrating self-organization. The NCR (bounded in red) and the 17 component cities (bounded in blue) are shown in Figure 1(a).

Brasilia was conceptualized because of the need to move the capital out of Rio de Janeiro to a more central location [26]; construction started in 1957, based on a winning plan by Lucio Costa. The portion of the BFD considered for the study is shown in Figure 1(b). On the other hand, the planning for the Australian capital started in 1901

https://doi.org/10.25088/ComplexSystems.30.3.273

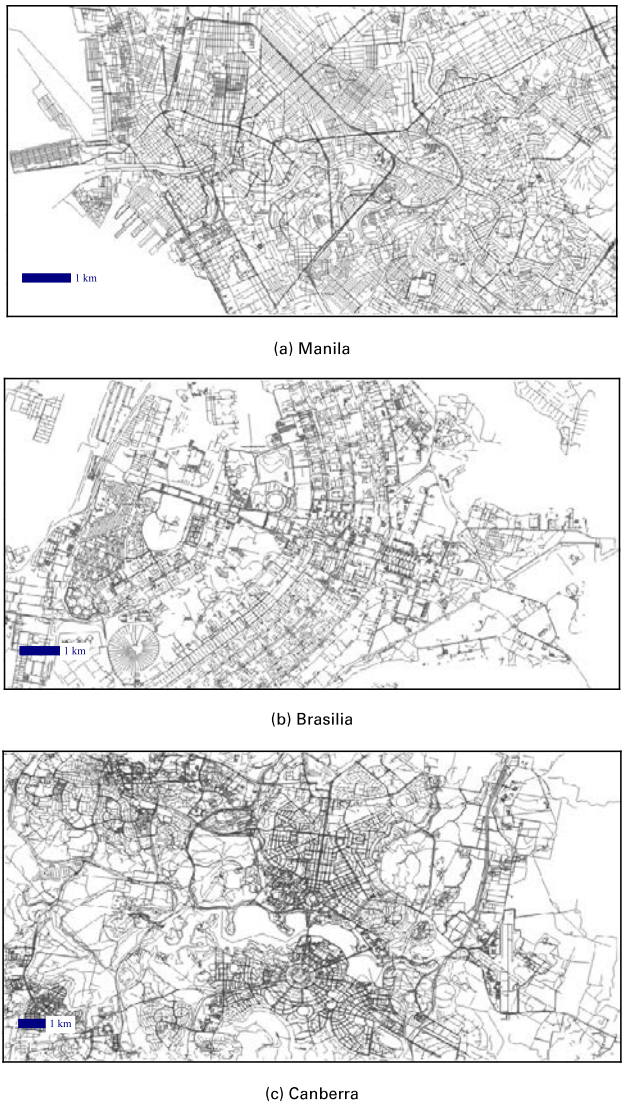

Figure 1. Map snapshots of datasets (relative scale provided: blue line denotes 1 km), focusing on the densest regions. (a) Metro Manila, Philippines, represents the self-organized cities (henceforth, the conurbation will be labeled as Manila). (b) The Brasilia Federal District, Brazil (henceforth, Brasilia), is one of the planned conurbations to be investigated. (c) The Australian Capital Territory, here focusing on Canberra, represents another strictly planned city (henceforth, Canberra).

[27, 28], with the location of the ACT selected in 1908 to be geographically between Sydney and Melbourne, then the two largest cities in Australia [29]. The design for the main city center, created by

Walter Burley Griffin and Marion Mahony Griffin and adapted in 1911, included carefully planned geometric patterns, a hallmark of centralized planning that is not easily observed in self-organized growth. The corresponding portion of the ACT around Canberra considered for the study is shown in Figure 1(c). Hereinafter, unless otherwise specified, we refer to the whole regions considered by the capital city names: Manila for the NCR, Brasilia for BFD and Canberra for ACT.

For all the capital areas considered, we extract the geographic information system (GIS) shapefiles of city boundaries and road networks from OpenStreetMap (OSM). We take in all roads as named by the city, which, in OSM, are reported as using a common ID. Additionally, we took all the reported roads from the data, including those that are used by pedestrians, as they, too, segment the space.

The shapefiles are processed using QGIS for extracting the relevant parameters for characterization. The individual roads are extracted as a set of node points containing the latitude ϕ and longitude θ coordinates with the same IDs. In this paper, our road network analyses are also constrained by the city boundaries; that is, for very long roads that stretch across different cities, we individually consider portions of the road bounded by each of the cities. The advantage of this segmentation within the city boundaries is the possibility for identifying the local configurations and conditions of the roads within the city limits.

For characterizing the segmented areas, we convert the road network map within the city boundaries into raster image files at scales of around $1:20\,000$. The images are analyzed via image processing techniques for obtaining the properties of each of the individual contiguous areas bounded by the streets. This method incorporates the fact that actual streets are not one-dimensional entities but occupy actual areas in space, and is thus deemed to be a better representative quantification of the space-filling functions of road networks.

2.2 Spatial Metrics for Characterization

As roads cut through space, two quantifiable morphological features are created that can be analyzed statistically: the *actual roads* and the *segmented blocks* bounded by the road crisscrossings. The most straightforward quantifiable measure for roads is the length L_r of an individual road r, which is heavily influenced not only by the separation distance between these points but also the prevailing intermediate geography between the two locations being connected. The processed OSM data allows for identifying the actual length of each of the roads within the city limits. The segmentation of the available area into blocks of different shapes and sizes, on the other hand, may be

https://doi.org/10.25088/ComplexSystems.30.3.273

quantified through the area A_b and perimeter P_b of each individual block b. Without doing actual survey on the ground, both A_b and P_b can be obtained within a reasonable level of uncertainty through pixel counts from the raster images obtained for each of the cities.

Some properties of the spatial elements cannot be derived straightforwardly but nevertheless give additional features for a more complete spatial characterization. For example, we can measure how roads wind through space due to the existing terrain. We adopt the inverse of the measure used by Stolum [30] for river meandering and define the inverse of the sinuosity, the straightness ξ_r of the road r, as

$$\xi_r = \frac{d_{0r}}{L_r} \quad 0 \le \xi_r \le 1 \tag{1}$$

with d_{0r} being the straight end-to-end length of the road. In this case, $\xi = 0$ represents closed loops and rotundas, while $\xi = 1$ is for straight roads. To our knowledge, this is one of the first applications of such a parameter to measure the winding tendency of the streets.

For a dimensionless characterization of blocks, previous authors have considered the shape factor ϕ_b as a dimensionless characterization metric to allow for statistical comparisons among different cities and across time [7, 9, 15]. The shape factor ϕ_b considers the ratio between the block area A_b and the square of the farthest distance between two points in the perimeter, D_b, scaled to range from 0 (thin strip) to 1 (perfect circle):

$$\phi_b = \frac{4}{\pi}\frac{A_b}{D_b^2}.$$

Here, as in a previous work [24], an equivalent dimensionless metric measuring the circularity σ_b is used,

$$\sigma_b = 4\pi\frac{A_b}{P_b^2} \tag{2}$$

where, again, $\sigma = 0$ denotes very thin strips and $\sigma = 1$ denotes a perfect circle. The circularity measure, which is one of the many possible metrics for describing the shape of a block [31–33], has distinct advantages that merits its use in our analyses. First, the computation of σ_b involves the actual measures obtained from the road network data: A_b is from the segmented block, and P_b is from the total actual road length for enclosing it. More importantly, σ captures the formation of dead-end roads within the blocks considered. Because the analyses are based on image processing, where the widths of the roads are accounted for, dead-end roads reduce the computed available area

inside a block, making it scale slower than the enclosing perimeter. We therefore expect cases where $\sigma \ll 1$; for example, for a circular block with reduced area due to dead-end roads. Figure 2 illustrates the different metrics used.

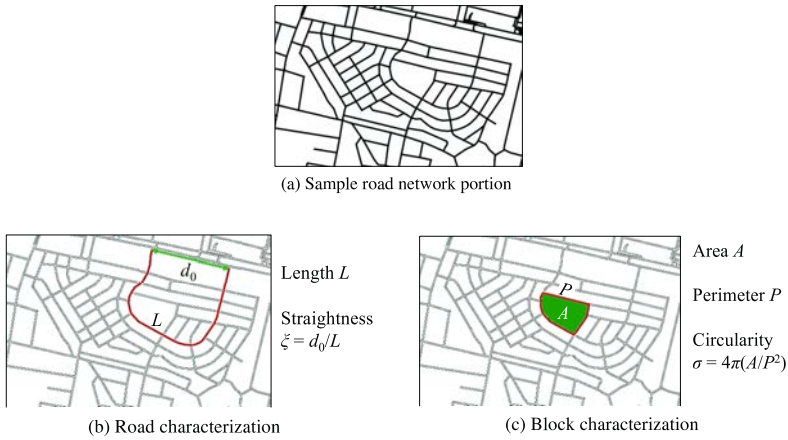

Figure 2. Illustrating the metrics used. (a) A sample portion of the road network, taken from a district in Quezon City, Metro Manila. (b) Each road is analyzed for its L and ξ, while (c) each block is characterized by its A, the bounding road segment P and σ.

3. Statistics of City Road Network Features

3.1 Road Metrics Distributions

In Figure 3(a) and (b), we present the statistics of L for the self-organized (Metro Manila) and planned (Brasilia and Canberra) cities, respectively. All $p(L)$ distributions show a unimodal behavior, with peaks at around $\hat{L} \approx 35$ m. Statistical tests based on the Kolmogorov–Smirnoff (KS) criterion [34, 35] reveal substantial non-normality of the distributions, with very large standard deviations suggesting fat-tailed behavior. Incidentally, due to the nature of the segmentation conducted in the Metro Manila conurbation [24], the statistics of street lengths in Figure 3(a) show shorter tails, in contrast with those of the planned cities.

Interestingly, despite the differences in the sizes of the cities considered, all the distributions appear to have similar modal street lengths $\hat{L}$, as can be seen from the combined plots in Figure 3(c). In fact, when the individual lengths are rescaled, say, by the square root of the city area, the distributions will begin to show stark differences.

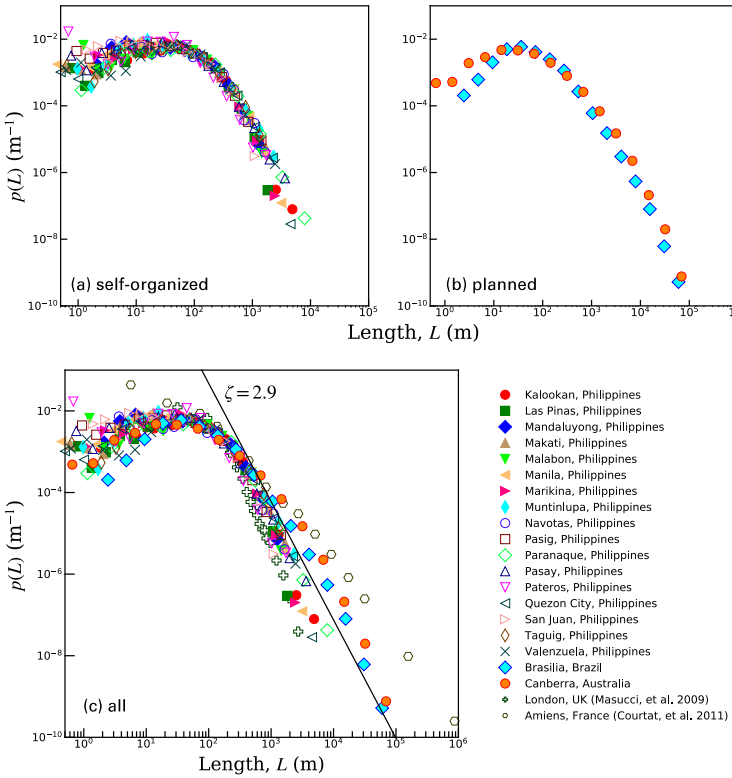

Figure 3. Road length distributions. The roads of the (a) self-organized cities of the Manila conurbation show a unimodal distribution with shorter tails than those of (b) planned cities, due to the city divisions. The unimodal distributions statistically deviate from a normal distribution. (c) When the distributions are plotted together, all show similar modal lengths at around $\hat{L} = 35$ km. A power-law $L^{-\gamma}$, with $\zeta = 2.9$, is shown near the tails region as a guide to the eye. Comparison with other datasets [8, 21] is also provided.

The fact that the road length distribution shows similar behavior regardless of the actual scale is an indication of the dominance of the local creation rules in their formation. The modal length $\hat{L}$ is deemed to be the optimal condition for road creation. Due to practical considerations, we expect a decreased incidence of even shorter roads, resulting in an initially increasing trend for $p(L)$ at $L < \hat{L}$. On the other hand, the finite extent of the cities also limits the possibility for creating longer roads, producing the corresponding decaying trend for $p(L)$ at the $L > \hat{L}$ regime. For this regime, we observe similar decay trends that are best parametrized by a decaying power-law $L^{-\gamma}$, where ζ is within the range of 2.4 to 2.9. The trend of $L^{-2.9}$ is shown in

Figure 3(c) as a guide to the eye. The substantial non-normality and fat-tailed behavior are expected; as a primary means of transport, there is a significant higher-than-random chance for a city to form very long roads. Incidentally, similar power-law tails are recovered for other datasets, such as the street networks of London, UK [8], and Amiens, France [21], also presented in Figure 3(c).

The similar underlying mechanisms in the formation of roads, resulting in the length distributions in Figure 3(c), are in agreement with the obtained universal statistics of road network distributions for the entire global road network [36]. Therefore, comparing road length probability density functions does not enable us to distinguish the effect of self-organization versus planning. To this end, we present in Figure 4(a)–(c) the distributions of the straightnesses ξ of each of the roads in the three city groups considered. The straightness is a dimensionless parameter, rescaled with the individual road's properties; as such, this parameter will be independent of the relative scales considered. Here, the effect of planning on an otherwise self-organized growth can be observed from the stark differences in the $p(\xi)$ trends.

As expected, roads are normally straight, as shown by the dominant peak near the $\xi = 1$ for all cities. Occasionally, we also find roundabouts and closed loops, represented by the secondary peak at $\xi = 0$. However, the effect of planning versus self-organized mechanisms is now readily discernible by looking at the other features of the $p(\xi)$ plots of Brasilia and Canberra. In Figure 4(b) and (c), we observe another characteristic value at $\xi \approx 0.3$ for the planned cities, a feature not observed for the self-organized setting of Manila. This may be explained by the fact that some roads are made to wind back to the original main street that they originate from, as illustrated in Figure 2(b), resulting in $\xi \approx 1/3$. In some cases, however, the streets follow a similar behavior observed for river systems. River systems may be viewed as the natural analog of streets, not only for their fractal geometries [37], but more importantly as transport avenues, in this case, for water from higher to lower elevations [38]. In a similar work, Stolum [30] observed that the meandering of rivers is a self-organized process that leads to a sinuosity, the inverse of the straightness $1/\xi$, approaching the value of π. Here, we observe the opposite: city roads, which are naturally designed to be straight under self-organized conditions to minimize travel time, can sometimes be made to be sinuous with planning. We surmise that under such conditions, the roads are made to follow the local topography, resulting in a sinuosity near the value of π. In Figure 4(d)–(f), we present portions of the conurbations considered to illustrate this result. The Manila road network is predominantly composed of straight segments with $\xi \to 1$. On the other hand, the Brasilia and Canberra road systems have been

https://doi.org/10.25088/ComplexSystems.30.3.273

designed to have roads having different sinuosities. These roads, upon closer inspection, are the ones that follow the natural topography and are mainly designed for pedestrians. The predominance of the roads that followed the natural contours results in the secondary peak at the $\xi = 1/\pi$ for their distributions.

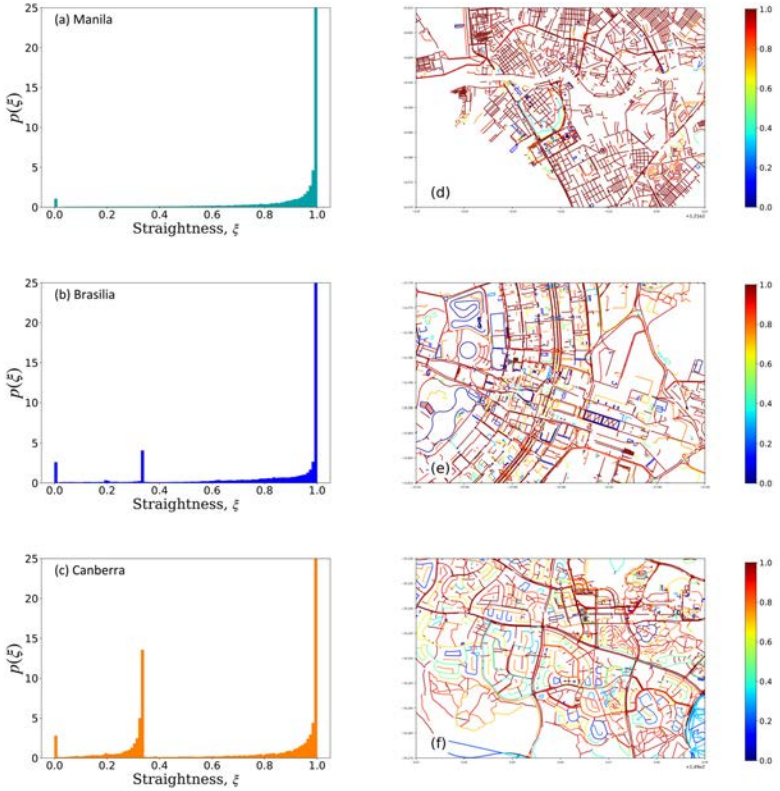

Figure 4. Road straightness distributions and sample snapshots. (a) The straightness of Manila roads, combining the results for all cities, shows distinct regions at $\xi = 0$ for roundabouts and $\xi = 1$ corresponding to straight roads. In contrast, roads in (b) Brasilia and (c) Canberra show a distinct peak at $\xi \approx 1/\pi$ as a result of planning. (d)–(f) The variations in the straightness values are depicted in the map segments for each of the cities.

3.2 Block Metrics Distributions

The obtained area and perimeter distributions from the analyses of high-resolution images of city snapshots are presented in Figure 5. Due to the scales of the images used, we were able to track segmented blocks even of very small areas, which we decided to include in the plots. For both self-organized and planned cities, we observe transitional regions where the plots show transitions in terms of the decay

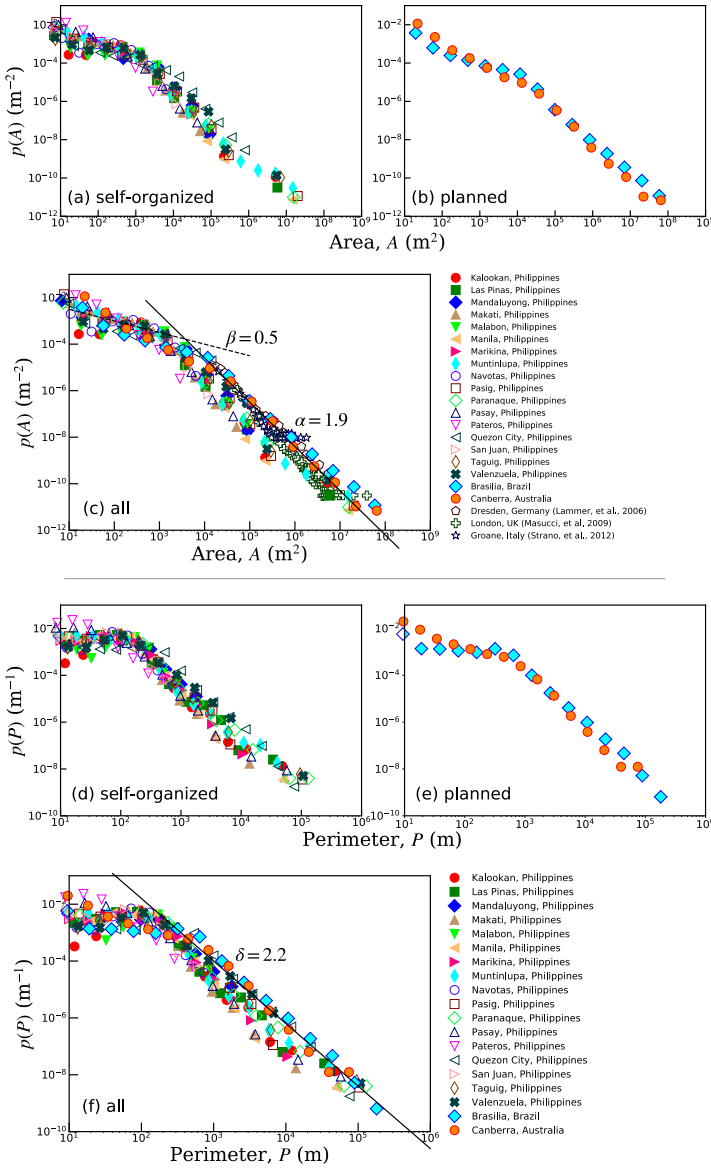

Figure 5. Block area and perimeter distributions. The distributions of areas A show dual-scaling behavior for both (a) self-organized and (b) planned urban areas. The area distributions are plotted together in (c), along with other datasets [8, 9] and the fit for the two power-law regimes: $A^{-\beta}$, where $\beta = 0.5$, for small A; and $A^{-\alpha}$, where $\alpha = 1.9$, for sufficiently large A. On the other hand, the perimeter distributions for (d) self-organized and (e) planned cities also follow fat-tailed statistics (f) best represented by the curve $P^{-\delta}$, with $\delta = 2.2$.

trends. Unlike the street length, however, these characteristic transition values are different for each of the cities considered.

Sufficiently large areas decay as a power-law, $p(A) \sim A^{-\alpha}$, where α is between 1.9 and 2.1, comparable to the observed decay trends for other city data [24, 39], such as Dresden, Germany [7], London, UK [8] (Figure 5(c)), and Groane, Italy [9] (Figure 5(c)), and in road network models [40]. Unlike previous works that neglected the small areas, however, we presented all the segmented areas collected by the algorithm up to the smallest scales resolved by the image analysis. As expected, the small-area distributions deviate from the steep power-law trend. These small areas are presented in Figure 5(c) with a power-law behavior, $p(A) \sim A^{-\beta}$ with β between 0.5 to 0.7. The lower scaling exponent is a consequence of the size limitations imposed by practical considerations. Beyond a particular value denoted by the knee of the distributions $p(A)$, the city blocks are too small to be of practical use. This results in the decreased incidence of very small blocks, parametrized here by the power-law with a lower scaling exponent.

Perimeter distributions also reveal similar trends, as illustrated in Figure 5. As expected, there is a general direct relationship between the block area and its bounding perimeter; larger blocks are expected to be bound by longer perimeters. We therefore expect two regimes in the $p(P)$ plots, corresponding to their counterparts in $p(A)$. Because of limitations in the very small perimeters, however, we did not find a general trend for the small P regimes; some perimeters are too small to be discriminated correctly. Instead, in Figure 5(f), we present the power-law fit for the tails of $p(P)$ that scales as $P^{-\delta}$, where δ is within the range 2.1 to 2.5, with $\delta = 2.2$ presented as a guide to the eye. The range of δ and the corresponding α suggests a scaling relation of approximately $P \sim A^{-\eta}$, with η ranging from 1.1 to 1.3. Interestingly, we find that the scaling exponents for L and P, which are both in linear dimensions, appear to be comparable, $\gamma \approx \delta$. This suggests that the linear cover of space is independent of the way it is measured, further hinting at the fractal nature of road network growth.

To simultaneously present the effects of A and P, we characterize the obtained blocks using the dimensionless circularity σ that measures their relative shapes. We present in Figure 6(a)–(c) the circularity distributions for the city conurbations considered, with the values for the regular polygons marked as a visual tool. One readily observes the modes around the σ values corresponding to triangular and square shapes, which is expected due to the grid-like nature of local roads. There is a finite, albeit relatively lower, occurrence probability of near-circular blocks, $\sigma \approx 1$. City road networks are not composed of isolated roundabouts; instead, to maximize connectivity, each

roundabout is expected to be accompanied by straight radial roads, thereby increasing the relative probability of finding noncircular blocks in the region. This high-σ regime of polygonal structures is an expected signature of road networks that is also found in other subject cities [7, 9]. Strano et al. [9] observed that the increased occurrence of regular, almost square-like blocks is a measure of homogenization: roads are formed to segment larger blocks into smaller patches with almost equal areas. Here, we believe that the same mechanisms had been at work, but at different time scales. The Manila conurbation, due to its self-organized nature, has slowly evolved into a homogenized state, while Brasilia and Canberra, drawn from master plans, have been homogenized since their formation.

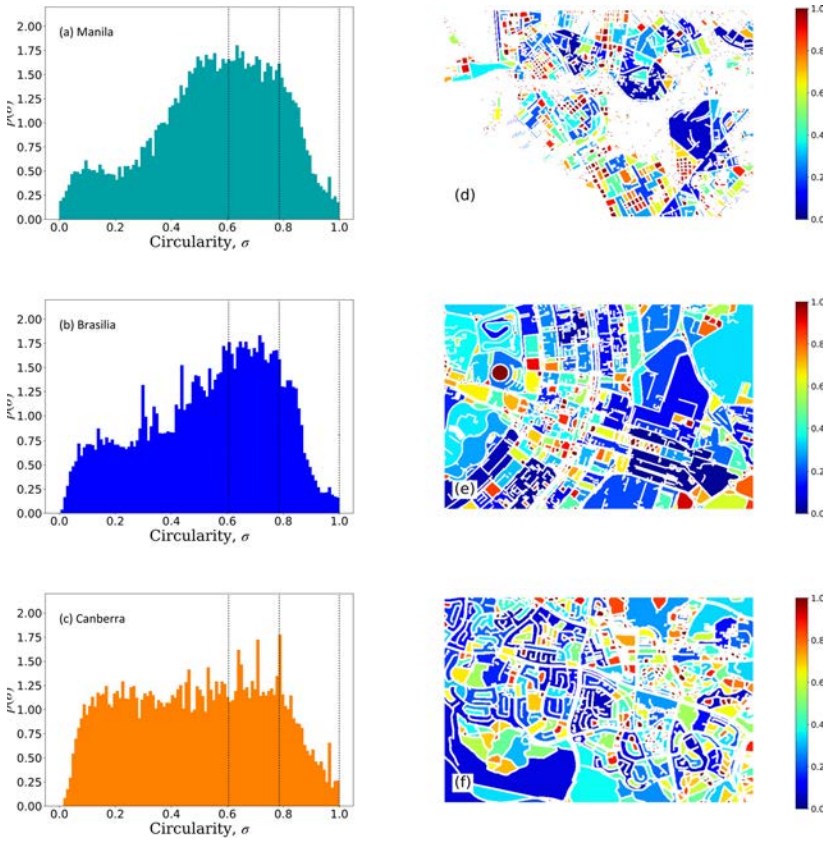

Figure 6. Block circularity distributions and sample snapshots. (a) The Manila conurbation shows a preponderance of near-triangular to square blocks, consistent with its grid-like nature. (b) Brasilia and (c) Canberra show more varied shapes. (d)–(f) Sample segments of the map showing the circularity values.

For all the distributions in Figure 6, we observe secondary peaks at very small σ values, corresponding to elongated polygons and/or fragmented areas with dead-end roads as captured by the image processing technique used. Such irregular patterns appear when there is a high density of almost-parallel roads in the same region. For Manila, we believe that this property resulted from its long self-organized evolution; additional roads are added to the metropolis as needed, due to the lack of coordinated central planning among the local governments. For Brasilia and Canberra, on the other hand, the occurrence of elongated and irregular shapes is deemed to be a result of a coordinated plan to recover a wide variation in the possible geometric figures resulting from the road intersections. In fact, the Canberra $p(\sigma)$ shown in Figure 6(c) shows a near-uniform distribution of all possible shapes. Barthelemy et al. [5] also observed the emergence of the lower-σ peak due to the incidences of elongated shapes in Paris, France, brought about by imposing strict intervention in road network construction over a self-organizing backdrop. In the lower panels of Figure 6(d)–(f), map sections for the same regions as in Figure 4(d)–(f) are presented to highlight these shape factor variations.

It is worth highlighting that the dimensionless road and block features, straightness and circularity, respectively, are interrelated, and their relationship is manifested in the obtained statistics. In Figure 4(a), we observe that the self-organized roads are mostly straight, $\xi = 1$; this results in the dominance of polygonal features, particularly between the regular triangular $\sigma = 0.604$ and square regions $\sigma = 0.785$ in Figure 6(a). On the other hand, Figure 4(b) and (c) reveal peaks at $\xi \approx 1/\pi$; the sinuous roads allow for a wider variation in possible shapes, as revealed by the relatively flatter circularity profiles in Figure 6(b) and (c). A visual comparison between road straightness profiles in Figure 4(d)–(f) and their corresponding block circularity maps in Figure 6(d)–(f) further highlights this correspondence.

4. Model of Road Network Growth

Road networks are examples of planar graphs, that is, graphs with no non-node link intersections. Previous works have used planar graphs as baselines by which real-world road networks are benchmarked. For example, Cardillo et al. [23] compared portions of street networks from various cities to minimum spanning trees (MST) and greedy triangulations (GT), the minimum and maximum links allowable, respectively, for regular planar graphs. On the other hand, Masucci et al. [8] considered both grid-like graphs and randomly

generated Erdos–Renyi planar graphs (ERPG) and growing random planar graphs (GRPG) for analyzing the London street network.

To be of practical value, however, models of street network construction need to mimic the possible realistic parameters on the ground. Barthelemy and Flammini [40] incorporated the idea of centers, or points of interest in space that need to be connected into the street network architecture. The model grows a street segment by minimizing the distance between several of the nearby centers, resulting in the formation of blocks observed in actual road networks. Courtat et al. [21] created a model for the morphogenesis of the street network of cities that dictates not just the evolution of the road network segments but also those of the urban centers, based on a few realistic rules.

Here, we build up from a previously proposed heuristic model of generating roads in space [24]. In simulating the growth of a city road network, we are guided by simple observations about the levels of planning and self-organization. In particular, longer roads are deemed to be more susceptible to local factors, particularly the local geographical conditions; as such, longer roads are less likely to produce regular geometric features in space. In contrast, shorter roads exploit the available areas left behind by the intersections of the longer, major roads; these roads, therefore, produce regular, almost grid-like patterns. In rare cases, large contiguous areas are being preserved and not cut into smaller blocks, such as industrial zones and parks and nature reserves; but for business and residential areas, small, regular grids are preferred.

With these observations in mind, we devise a two-step model for road network growth as illustrated in Figure 7. Self-organized growth of long roads begins with initial random seed points in two-dimensional space. At any given time, an origin and destination point pair is selected, labeled as **A** and **B**, respectively, in Figure 7(a). By introducing a destination point, the model incorporates a global bearing in the formation of a road. Locally, however, the model relies on a k-nearest-neighbor-based routing scheme. The routing algorithm selects the yet unconnected k nearest neighbors of the origin and computes each of their distances to the destination. A road segment is created toward the nearest neighbor that is closest to the destination; this new node then becomes the new origin, and the process is repeated until the destination is reached. Doing this procedure iteratively for different sets of **A** and **B** will eventually cover the entire set of points.

This, in turn, creates a primary network with closed loops that have irregular shapes. The second part of the model, schematically illustrated in Figure 7(b), selects closed loops, which are then altered to have grid-like structures with directionalities following the major axes of the shape being considered. The procedure is deemed to

https://doi.org/10.25088/ComplexSystems.30.3.273

represent the planned formation of business areas and residential settlements in modern cities. In contrast with previous models with well-defined points for connectivity that ensure planarity (i.e., no intersection) at all times, our model allows for the grid-like structures to sometimes intersect with pre-existing portions of the major roads, creating new intersections in the process. This is deemed to be at work in self-organizing cities, like the Metro Manila dataset from our work.

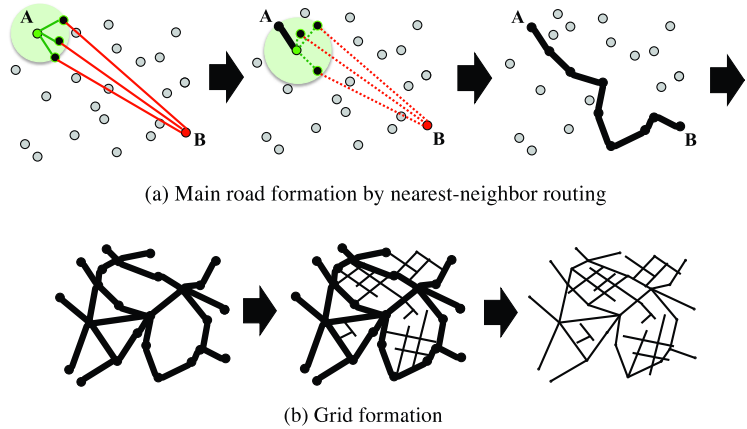

(a) Main road formation by nearest-neighbor routing

(b) Grid formation

Figure 7. Model of road network development. (a) Nearest-neighbor routing: starting with an origin (green) and a destination point (red), the model looks for the k nearest neighbors of the origin, in this case for $k = 3$. A road segment is created toward the nearest neighbor that is closest to the destination. Repeating the process will eventually create the road connecting the origin and destination points. (b) Grid formations: out of the closed loops formed by the nearest-neighbor routing algorithm, grid-type roads are constructed along the major axes of the closed loops.

The model is tracked for varying parameters, particularly the number of original points N, the number of main-road connections to be made M, and nearest-neighbor k for the main road routing algorithm. Moreover, for the grid-type connections, we use the variable R as the number of regions where grid-like branching will occur. Every grid-like formation is guided by the stochastic variable $Q \in [0, 5]$, the number of roads that will be formed in a particular branching region, and $\ell \in [0, L/10]$, the length of a road, with $L = 5000$ set as the arbitrary dimension of the square region where the roads are generated. Figure 8 shows representative networks generated for varying N, M and R parameter values.

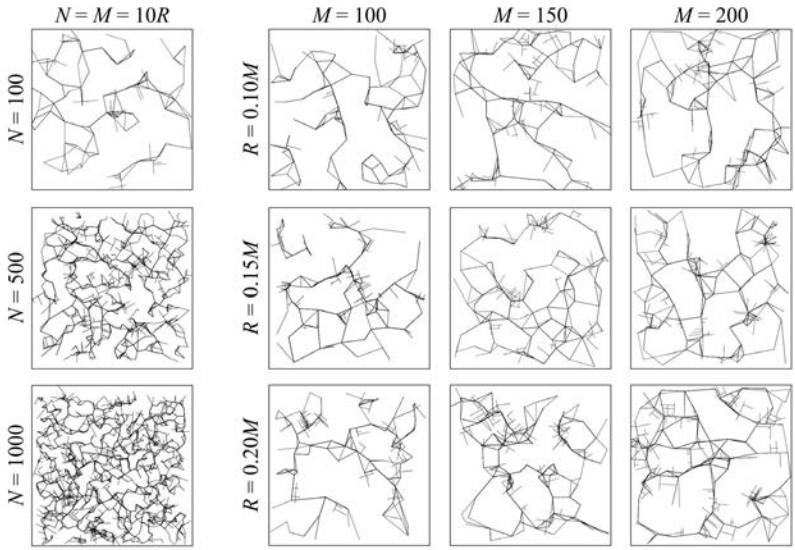

Figure 8. Representative model results. The first column shows that increasing N only decreases the possibility for finding larger areas, as expected. For a fixed value of N, we present in succeeding columns the representative road network generated for different M and R pairs.

For a finite L, the effect of increasing N is to decrease the maximum possible block area, as shown in the first column of Figure 8. As such, we use the smallest value of $N = 100$ for tracking the effects of M and N, which are shown here on the right panels. Qualitatively, increasing M increases the connectivity of the points, reducing the incidence of isolated "islands" of subnetworks. On the other hand, the parameter R controls the density of grid-like patterns, as expected. For each of the parameter sets presented in the figure, we obtain the statistical distributions of the block metrics described in Section 2.2 to find the similarities and differences with those of real road networks. These distributions are presented in Figure 9.

For the case of $N = 100$ in an $L \times L = 5000 \times 5000$ space, the nearest-neighbor routing rule produces dual-scaling behavior in $p(A)$ similar to that observed in the empirical street data. At small areas, $p(A) \sim A^{-\beta_m}$, with $\beta_m \approx 0.8$, slightly higher than $\beta \approx 0.5$ in empirical data. On the other hand, for larger areas, $p(A) \sim A^{-\alpha_m}$ with $\alpha_m \approx 1.5$, this time lower than $\alpha \approx 1.9$. Increasing the number of points N where connections can be made results in a fragmentation of the available space into many smaller areas. Because of this, the incidence of smaller areas increases, and the regime of the less steep power-law is

https://doi.org/10.25088/ComplexSystems.30.3.273

diminished, as shown in Figure 9(a). Incidentally, within the range of the parameters M and R considered, no significant difference is observed for the $p(A)$, as can be observed in Figure 9(b) and (c). The fact that the model shows a similar knee behavior with differing power-law trends is indicative of a mechanism inherent in city road formations. The model clearly illustrates that the lower exponent in the small-area power-law regime emerges due to the incomplete fragmentation of the space due to the road networks. In the real world, this regime is still observed despite the continuous growth and evolution of a city due to practical considerations; that is, at some point, it would be impractical and inefficient to further subdivide the space into very tiny areas.

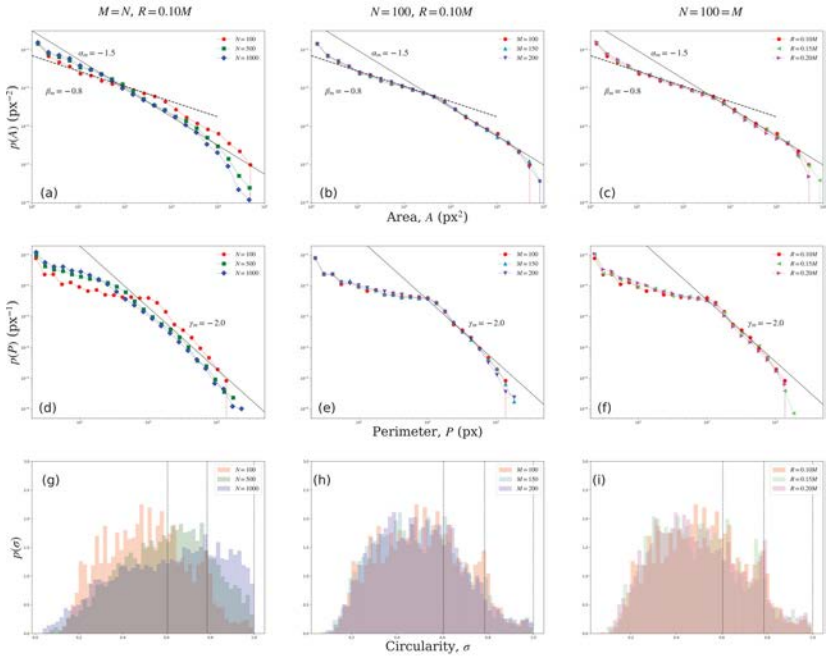

Figure 9. Model roads and blocks statistics. In the first column, increasing N results in homogenization, (a) removing the knee region in $p(A)$ and (b) in $p(P)$, and (c) broadening of the $p(\sigma)$. For a fixed $N = 100$, the M and R values considered did not produce significant effects. (b)–(c) The $p(A)$ show dual scaling regimes $p(A) \sim A^{-\beta_m}$ for small A and $p(A) \sim A^{-\alpha_m}$ for large A, where $\beta_m \approx 0.8$ and $\alpha_m \approx 1.5$. (e)–(f) The corresponding $p(P)$ is fitted with a power-law tail $p(P) \sim P^{-\delta_m}$, with $\delta_m \approx 2.0$. (h)–(i) The $p(\sigma)$ is affected by R, with a pronounced peak at the square circularity for higher R values.

The same mechanisms are believed to be responsible for the perimeter distributions $p(P)$, shown in Figure 9(d)–(f). The tails of the distributions appear to obey the power-law trend $p(P) \sim P^{-\delta_m}$ with $\delta_m \approx 2.0$, slightly lower than the obtained δ for the city road networks that range from 2.1 to 2.5. As increasing N fragments the available space into smaller pieces, the less steep regions of the $p(P)$ plot are slowly being diminished and the power-law tail dominates.

Finally, in Figure 9(g)–(i), we present the circularity distributions of the model. The effect of N is to broaden the distribution of σ; as space is further subdivided, more variations in space emerge, including the small, elongated portions also observed in the cities, as highlighted in Figure 9(g). As expected, the effect of the grid formations R is to increase the square-like regions, as shown by the marked regime in Figure 9(i).

5. Conclusion

The availability of fast and efficient computational tools has allowed for quantitative examinations of large-scale complex systems such as city road networks. Despite the complex processes involved in the actual growth of a road network, we have shown, using a combination of geographic information system (GIS) analyses and image processing of how roads spread in space, how representative cities across different backgrounds show similarities and differences in terms of their spatial statistics. The length of roads, and areas and perimeters of blocks all exhibit fat tails that may be approximated as power-laws, suggesting a significantly higher chance (than random) of finding long roads and big areas, consistent with practical considerations. Because of the similarities obtained, these first-level characterization metrics are not a good means to distinguish self-organized and planned conditions; the characteristic road length and block area are the same across all regions. In contrast, the dimensionless metrics straightness (for roads) and circularity (for blocks) highlight the effect of planning over self-organization. Self-organized cities tend to favor straight roads while planned ones follow the contour, resulting in sinuous roads with sinuosities approaching π; as a result, self-organized blocks are predominantly composed of regular polygonal structures, while planned blocks have more varied shapes. Finally, a simple model that creates main roads via nearest-neighbor routing and grid-like blocks at random seed points has recovered the nontrivial features of the obtained road network statistics and has given insights on the nature of road network formation.

https://doi.org/10.25088/ComplexSystems.30.3.273

Studies such as this one add to a growing literature of quantitative characterizations of urban spatial patterns, like the ones done in Dresden, Germany, and other German cities [7]; Paris [5], Amiens and other cities [21] in France; Milan in Italy [9]; and London in the United Kingdom [6, 8, 15, 16]. Our focus on a different set of data, particularly that of Manila, which is one of the emerging megacities in Asia [41] characterized by rapid growth and development over the past few decades [42], adds an entirely different geographical and economic layer into the current state of urban road network analyses, and therefore complements previous efforts to find underlying quantifiable features of urbanization. Moreover, a study on completely planned cities may be useful as a benchmark for future developments in new and emerging urban centers, as the road network architectures of these cities are static; useful spatial features may also be applied in developing new growth centers [43]. Our model results also show that the seemingly complicated features emergent on city road patterns can be replicated using a simple model derived from basic considerations.

Our work aims to present a specific example rather than a generalization of the complementary effects of self-organizing and strictly planned factors in the growth of road networks. In particular, it extends our previous work [24] that results in mostly winding roads, which best represents the early exploration stages [9]. By adding the formation of grid-like blocks in the available space, we were also able to capture the densification stage [9], and, in turn, the resulting nontrivial regimes in the road length and block area distributions.

We acknowledge that more complex mechanisms, which may be specific to a particular city, are at play in the development of urban zones. Still, the proposed characterization based on purely spatial metrics may provide a useful guide for further analyses of growing urban landscapes, and may even reveal features unique for a particular case being studied [44]. While we considered the case of strong central planning and very loose self-organization, we believe that far more interesting results are expected for cities that are midway between these two extremes. Finally, our proposed model, which, when applied, effectively decouples the inherent self-organization and planning in road formations, may provide a simple parametrization for the process of urban growth.

Acknowledgments

M. T. Cirunay sincerely acknowledges the Science Education Institute of the Department of Science and Technology (DOST-SEI), Philippines, through the De La Salle University, for the financial support

through the Accelerated Science and Technology Human Resource Development Program (ASTHRDP) Scholarship.

References

[1] L. M. A. Bettencourt, J. Lobo, D. Helbing, C. Kühnert and G. B. West, "Growth, Innovation, Scaling, and the Pace of Life in Cities," *Proceedings of the National Academy of Sciences*, **104**(17), 2007 pp. 7301–7306. doi:10.1073/pnas.0610172104.

[2] S. A. Ahmad, "Urbanization, Energy Consumption and Entropy of Metropolises," *Complex Systems*, **28**(3), 2019 pp. 287–312. doi:10.25088/ComplexSystems.28.3.287.

[3] A. V. Moudon, *Built for Change: Neighborhood Architecture in San Francisco*, Cambridge, MA: MIT Press, 1986.

[4] M. Batty, *Cities and Complexity: Understanding Cities with Cellular Automata, Agent-Based Models, and Fractals*, Cambridge, MA: MIT Press, 2005.

[5] M. Barthelemy, P. Bordin, H. Berestycki and M. Gribaudi, "Self-Organization versus Top-Down Planning in the Evolution of a City," *Scientific Reports*, **3**(1), 2013 2153. doi:10.1038/srep02153.

[6] A. P. Masucci and C. Molinero, "Robustness and Closeness Centrality for Self-Organized and Planned Cities," *The European Physical Journal B*, **89**(2), 2016 53. doi:10.1140/epjb/e2016-60431-2.

[7] S. Lämmer, B. Gehlsen and D. Helbing, "Scaling Laws in the Spatial Structure of Urban Road Networks," *Physica A: Statistical Mechanics and Its Applications*, **363**(1), 2006 pp. 89–95. doi:10.1016/j.physa.2006.01.051.

[8] A. P. Masucci, D. Smith, A. Crooks and M. Batty, "Random Planar Graphs and the London Street Network," *The European Physical Journal B*, **71**(2), 2009 pp. 259–271. doi:10.1140/epjb/e2009-00290-4.

[9] E. Strano, V. Nicosia, V. Latora, S. Porta and M. Barthélemy, "Elementary Processes Governing the Evolution of Road Networks," *Scientific Reports*, **2**(1), 2012 296. doi:10.1038/srep00296.

[10] M. Batty and P. A. Longley, *Fractal Cities: A Geometry of Form and Function*, San Diego, CA: Academic Press, 1994.

[11] P. Frankhauser, "The Fractal Approach. A New Tool for the Spatial Analysis of Urban Agglomerations," *Population: An English Selection*, **10**(1), 1998 pp. 205–240. www.jstor.org/stable/2998685.

[12] M. L. De Keersmaecker, P. Frankhauser and I. Thomas, "Using Fractal Dimensions for Characterizing Intra-urban Diversity: The Example of Brussels," *Geographical Analysis*, **35**(4), 2003 pp. 310–328. doi:10.1111/j.1538-4632.2003.tb01117.x.

[13] Y. Chen and J. Wang, "Describing Urban Evolution with the Fractal Parameters Based on Area-Perimeter Allometry," *Discrete Dynamics in Nature and Society*, **2016**, 2016 4863907. doi:10.1155/2016/4863907.

[14] M. T. Cirunay, M. N. Soriano and R. C. Batac, "Analysis of the Road Network Evolution through Geographical Information Extracted from Historical Maps: A Case Study of Manila, Philippines," *Journal of Advances in Information Technology*, **10**(3) 2019 pp. 114–118. doi:10.12720/jait.10.3.114-118.

[15] A. P. Masucci, K. Stanilov and M. Batty, "Limited Urban Growth: London's Street Network Dynamics since the 18th Century," *PLOS ONE*, **8**(8), 2013 e69469. doi:10.1371/journal.pone.0069469.

[16] R. Murcio, A. P. Masucci, E. Arcaute and M. Batty, "Multifractal to Monofractal Evolution of the London Street Network," *Physical Review E*, **92**(6), 2015 062130. doi:10.1103/PhysRevE.92.062130.

[17] S. Porta, P. Crucitti and V. Latora, "The Network Analysis of Urban Streets: A Dual Approach," *Physica A: Statistical Mechanics and Its Applications*, **369**(2), 2006 pp. 853–866. doi:10.1016/j.physa.2005.12.063.

[18] B. Jiang, "A Topological Pattern of Urban Street Networks: Universality and Peculiarity," *Physica A: Statistical Mechanics and Its Applications*, **384**(2), 2007 pp. 647–655. doi:10.1016/j.physa.2007.05.064.

[19] I. Mishkovski, M. Biey and L. Kocarev, "Vulnerability of Complex Networks," *Communications in Nonlinear Science and Numerical Simulations*, **16**(1), 2011 pp. 341–349. doi:10.1016/j.cnsns.2010.03.018.

[20] C. Ducruet and L. Beauguitte, "Spatial Science and Network Science: Review and Outcomes of a Complex Relationship," *Networks and Spatial Economics*, **14**(3), 2014 pp. 297–316. doi:10.1007/s11067-013-9222-6.

[21] T. Courtat, C. Gloaguen and S. Douady, "Mathematics and Morphogenesis of Cities: A Geometrical Approach," *Physical Review E*, **83**(3), 2011 036106. doi:10.1103/PhysRevE.83.036106.

[22] J. F. Valenzuela, E. F. Legara, X. Fu, R. S. M. Goh, R. De Souza and C. Monterola, "A Network Perspective on the Calamity, Induced Inaccessibility of Communities and the Robustness of Centralized, Landbound Relief Efforts," *International Journal of Modern Physics C*, **25**(6), 2014 1450047. doi:10.1142/S0129183114500478.

[23] A. Cardillo, S. Scellato, V. Latora and S. Porta, "Structural Properties of Planar Graphs of Urban Street Patterns," *Physical Review E*, **73**(6), 2006 066107. doi:10.1103/PhysRevE.73.066107.

[24] M. T. Cirunay and R. C. Batac, "Statistical Signatures of the Spatial Imprints of Road Network Growth," *International Journal of Modern Physics C*, **29**(10), 2018 1850099. doi:10.1142/S0129183118500997.

[25] Y. Boquet, "From Paris and Beijing to Washington and Brasilia: The Grand Design of Capital Cities and the Early Plans for Quezon City," *Philippine Studies: Historical and Ethnographic Viewpoints*, **64**(1), 2016 pp. 43–71. www.jstor.org/stable/26621882.

[26] G. N. Batista, S. Ficher, F. Leitão and D. A. de França, "Brasilia: A Capital in the Hinterland," *Planning Twentieth Century Capital Cities* (D. Gordon, ed.), London: Routledge, 2006.

[27] L. Wigmore, *Canberra: History of Australia's National Capital*, 2nd ed., Canberra: Dalton Publishing Company, 1972.

[28] *The Canberra Spatial Plan*, Canberra: Australian Capital Territory Planning and Land Authority, 2004.

[29] C. Vernon, "Canberra: Where Landscape Is Pre-eminent," *Planning Twentieth Century Capital Cities* (D. Gordon, ed.), London: Routledge, 2006.

[30] H.-H. Stolum, "River Meandering as a Self-Organization Process," *Science*, **271**(5256), 1996 pp. 1710–1713. doi:10.1126/science.271.5256.1710.

[31] J. Bogaert, R. Rousseau, P. Van Hecke and I. Impens, "Alternative Area-Perimeter Ratios for Measurement of 2D Shape Compactness of Habitats," *Applied Mathematics and Computation*, **111**(1), 2000 pp. 71–85. doi:10.1016/S0096-3003(99)00075-2.

[32] E. Bribiesca, "An Easy Measure of Compactness for 2D and 3D Shapes," *Pattern Recognition*, **41**(2), 2008 pp. 543–554. doi:10.1016/j.patcog.2007.06.029.

[33] R. Montero and E. Bribiesca, "State of the Art of Compactness and Circularity Measures," *International Mathematical Forum*, **4**(27), 2009 pp. 1305–1335.

[34] A. Clauset, C. R. Shalizi and M. E. J. Newman, "Power-Law Distributions in Empirical Data," *SIAM Review*, **51**(4), 2009 pp. 661–703. doi:10.1137/070710111.

[35] J. Alstott, E. Bullmore and D. Plenz, "powerlaw: A Python Package for Analysis of Heavy-Tailed Distributions," *PLOS ONE*, **9**(1), 2014 e85777. doi:10.1371/journal.pone.0085777.

[36] E. Strano, A. Giometto, S. Shai, E. Bertuzzo, P. J. Mucha and A. Rinaldo, "The Scaling Structure of the Global Road Network," *Royal Society Open Science*, **4**(10), 2017 170590. doi:10.1098/rsos.170590.

[37] B. B. Mandelbrot, *The Fractal Geometry of Nature*, New York: W. H. Freeman, 1983.

[38] M. Barthélemy, "Spatial Networks," *Physics Reports*, **499**(1), 2011 pp. 1–101. doi:10.1016/j.physrep.2010.11.002.

[39] R. Louf and M. Barthélemy, "A Typology of Street Patterns," *Journal of Royal Society Interface*, **11**(101), 2014 20140924. doi:10.1098/rsif.2014.0924.

[40] M. Barthélemy and A. Flammini, "Modeling Urban Street Patterns," *Physical Review Letters*, **100**(13), 2008 138702. doi:10.1103/PhysRevLett.100.138702.

[41] B. Wehrmann, "Land Development Strategies in Megacities: Guiding Land Use and Land Rights in the Context of Urban Sprawl and Informality," in *Megacities: Our Global Urban Future* (F. Kraas, S. Aggarwal, M. Coy and G. Mertins, eds.), Dordrecht: Springer, 2014 pp. 75–80. doi:10.1007/978-90-481-3417-5_6.

[42] *Philippine Economic Update: Making Growth Work Better for Small Business*, Report No. 99648-PH, The World Bank Group in the Philippines, 2015.

[43] S. Derrible, "Complexity in Future Cities: The Rise of Networked Infrastructure," *International Journal of Urban Sciences*, **21**(sup1), 2017 pp. 68–86. doi:10.1080/12265934.2016.1233075.

[44] M. T. Cirunay, M. N. Soriano and R. C. Batac, "Preserved Layout Features Embedded in Road Network Development," *Journal of Physics: Complexity*, **1**(1), 2020 015004. doi:10.1088/2632-072X/ab7f4e.